

Low Complexity Artificial Noise Aided Beam Focusing Design in Near-Field Terahertz Communications

Zhifeng Tang, *Member, IEEE*, Nan Yang, *Senior Member, IEEE*, Xiangyun Zhou, *Fellow, IEEE*, Salman Durrani, *Senior Member, IEEE*, Markku Juntti, *Fellow, IEEE*, and Josep Miquel Jornet, *Fellow, IEEE*

Abstract—In this paper, we develop a novel low-complexity artificial noise (AN) aided beam focusing scheme in a near-field terahertz wiretap communication system. In this system, the base station (BS) equipped with a large-scale array transmits signals to a legitimate user, while mitigating information leakage to an eavesdropper. We formulate an optimization problem to maximize the secrecy rate achieved at the legitimate user and solve it by designing the optimal beam focusing and power allocation. Numerical results demonstrate the significant performance improvement achieved by the proposed AN aided beam focusing scheme, especially when the eavesdropper is located closer to the BS than the legitimate user.

Index Terms—Physical layer security, near-field terahertz communications, artificial noise, beam focusing.

I. INTRODUCTION

With the growing demand for ultra-fast and massive data transmission, terahertz (THz) communications has emerged as a game-changing technology for the sixth-generation (6G) wireless networks [1]. In particular, THz communications operates in the THz frequency range, i.e., 0.1–10 THz, offering extensive spectrum and enabling picosecond-level symbol duration [2]. With ultrabroad bandwidth and ultra-high data rate, THz communications unlocks rich opportunities for the Internet of Things (IoT) applications, such as ultra-fast data transfer in wireless data centers [3].

It is noted that the Rayleigh distance in THz communication systems can be significantly larger than that at lower frequencies, due to the short wavelength of THz propagation and the use of large-scale antenna arrays in such systems, which results in a large near-field region [4]. This large region offers enhanced physical layer security by confining the signal to a smaller spatial area, thus limiting the potential for interception by unauthorized users. However, a high risk of information leakage to nearby eavesdroppers still remains [5]. In light of this, [6] proposed a near-field point-to-point transmission framework and a beamformer to optimize the secrecy rate. Also, [6] revealed that the near-field secrecy performance primarily relies on the distance disparity between the legitimate user and the eavesdropper. In [7], an extended multi-user near field communication system was introduced,

This work was supported by the Australian Research Council Discovery Project (DP230100878).

Z. Tang, N. Yang, X. Zhou, and S. Durrani are with the School of Engineering, Australian National University, Canberra, ACT 2601, Australia (Emails: {zhifeng.tang, nan.yang, xiangyun.zhou, salman.durrani}@anu.edu.au).

Markku Juntti is with the Centre for Wireless Communications, University of Oulu, Oulu 90014, Finland (Email: markku.juntti@oulu.fi).

Josep Miquel Jornet is with the Department of Electrical and Computer Engineering, Northeastern University, Boston, MA 02120, USA (Email: j.jornet@northeastern.edu).

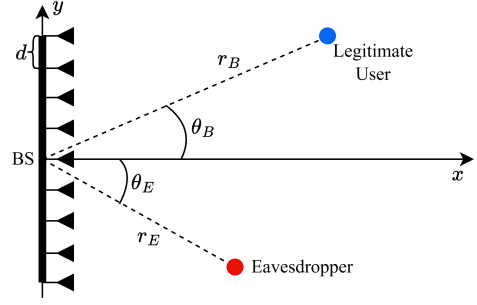


Fig. 1. Illustration of our considered near-field communication system.

where hybrid beamforming was developed based on successive convex approximation and optimization to maximize the minimum secrecy rate among all legitimate users. A wavefront hopping scheme was proposed in [8] to decrease the probability of message eavesdropping. In addition, the nullspace artificial noise (AN) of the legitimate channel was proposed in [9] to improve the secrecy rate. Although the aforementioned studies have presented effective methods to improve the secrecy performance in near-field communication systems, these methods introduced high computational complexity, especially when THz communication systems deploy extremely large-scale arrays, which brings huge challenges for practical implementation. Very recently, an AN aided beam focusing scheme was proposed in [10], which effectively reduces computational complexity while achieving limited secrecy gains. To further improve the secrecy performance with low computational complexity, we will devise a novel AN aided beam focusing scheme, motivating this work.

In this letter, we consider the downlink in a near-field THz wiretap communication system, where a base station (BS) transmits signals to a legitimate user while an eavesdropper exists in the system to wiretap the transmission. Inspired by AN aided beam focusing design [10], we develop a novel low-complexity AN aided beam focusing scheme to improve the secrecy performance. In particular, aided by approximation techniques, we first decouple the secrecy rate optimization problem into separate signal and AN beam focusing subproblems and solve each subproblem by a low-complexity one-dimensional search method, while considering their combined impact on both the legitimate user and the eavesdropper. We then derive the closed-form expression for the optimal power allocation ratio on AN transmission to maximize the secrecy rate. Through numerical results, we demonstrate that our proposed scheme achieves profound secrecy rate improvement compared to the existing ones.

II. SYSTEM MODEL

We consider the downlink of a near-field THz wiretap communication system, as depicted in Fig. 1. In this system, a BS transmits signals to a legitimate user, while one eavesdropper exists to wiretap this signal. We assume that both the legitimate user and the eavesdropper are standard low-cost system users (e.g., sensors in THz IoT applications), while the eavesdropper is unauthorized to access the signal transmitted to the legitimate user in the considered transmission. The BS

employs a uniform linear large-scale array with N antenna elements, while the legitimate user and the eavesdropper are single antenna receivers [9]–[11]. We assume that the legitimate user and the eavesdropper are located in the near-field region, i.e., at distances smaller than the Rayleigh distance, given by $d_R = 2D^2/\lambda$, but greater than the Fresnel distance, given by $d_F = 0.62\sqrt{D^3/\lambda}$, where D is the antenna aperture size of the BS and λ is the wavelength. Moreover, we assume that the perfect channel state information of the legitimate user and the eavesdropper is available at the BS via effective near-field channel estimation and beam training methods, such as those in [12], [13].

A. Channel Model

Without loss of generality, we assume that the large-scale array is placed along the y -axis, while the center of the large-scale array is located at the origin, i.e., $(0, 0)$. Accordingly, the n th antenna element, $n \in \{1, \dots, N\}$, has the coordinate $(0, \delta_n d)$, where $\delta_n = n - \frac{N-1}{2}$ and d represents the spacing between adjacent antenna elements. Moreover, the coordinates of the legitimate user and the eavesdropper are given by $L_B = (r_B \cos \theta_B, r_B \sin \theta_B)$ and $L_E = (r_E \cos \theta_E, r_E \sin \theta_E)$, respectively, where r_B and r_E denote the radial distance of the legitimate user and the eavesdropper from the origin, respectively, and θ_B and θ_E denote the spatial angle from the x -axis to the legitimate user and the eavesdropper, respectively. As such, the distances from the n th antenna element of the large-scale array to the legitimate user and the eavesdropper are expressed as

$$r_{n,B} = \sqrt{r_B^2 + (\delta_n d)^2 - 2r_B \delta_n d \sin \theta_B} \quad (1)$$

and

$$r_{n,E} = \sqrt{r_E^2 + (\delta_n d)^2 - 2r_E \delta_n d \sin \theta_E}, \quad (2)$$

respectively.

In near-field communications, the multipath channel model is usually adopted, which consists of a line-of-sight (LoS) path and several non-LoS (NLoS) paths. However, due to the severe path loss in the NLoS channel and low antenna gain at the receiver, the received power of NLoS paths is negligible compared to that of the LoS path [4]. Thus, the near-field channel from the BS to the legitimate user and the eavesdropper can be approximated as

$$\mathbf{h}_B^H \approx h_{B,\text{LoS}} \mathbf{h}^H(r_B, \theta_B) \quad (3)$$

and

$$\mathbf{h}_E^H \approx h_{E,\text{LoS}} \mathbf{h}^H(r_E, \theta_E), \quad (4)$$

respectively, where $h_{B,\text{LoS}} = \frac{\lambda}{4\pi r_B} \exp(-\frac{1}{2}K(f)r_B)$ and $h_{E,\text{LoS}} = \frac{\lambda}{4\pi r_E} \exp(-\frac{1}{2}K(f)r_E)$ denote the large-scale path loss from the origin to the legitimate user and the eavesdropper, respectively, $K(f)$ is the molecular absorption coefficient at frequency f , and $\mathbf{h}(r_B, \theta_B)$ and $\mathbf{h}(r_E, \theta_E)$ are the channel steering vectors, given by

$$\mathbf{h}^H(r_B, \theta_B) = [e^{-j2\pi r_{1,B}}, \dots, e^{-j2\pi r_{N,B}}] \quad (5)$$

and

$$\mathbf{h}^H(r_E, \theta_E) = [e^{-j2\pi r_{1,E}}, \dots, e^{-j2\pi r_{N,E}}], \quad (6)$$

respectively.

B. Signal Model

We assume that the BS transmits the information-carrying signal along with the AN to serve the legitimate user while disrupting the eavesdropper. We denote $\mathbf{x} \in \mathbb{C}^N$ as the signal vector transmitted from the BS to the legitimate user, given by $\mathbf{x} = \mathbf{w}_s s + \mathbf{w}_z z$, where $\mathbf{w}_s \in \mathbb{C}^N$ denotes the beam focusing vector of the signal, s denotes the information-carrying signal for the legitimate user, $\mathbf{w}_z \in \mathbb{C}^N$ denotes AN vector, and z denotes the AN. Hence, the received signals at the legitimate user and the eavesdropper are given by

$$y_B = \mathbf{h}_B^H (\mathbf{w}_s s + \mathbf{w}_z z) + n_B \quad (7)$$

and

$$y_E = \mathbf{h}_E^H (\mathbf{w}_s s + \mathbf{w}_z z) + n_E, \quad (8)$$

respectively, where $n_B \sim \mathcal{CN}(0, \sigma_B^2)$ and $n_E \sim \mathcal{CN}(0, \sigma_E^2)$ denote the additive white Gaussian noise (AWGN) at the legitimate user and the eavesdropper, respectively. Here, we assume that the legitimate user and the eavesdropper have the same noise power, i.e., $\sigma_B^2 = \sigma_E^2 = \sigma^2$. According to (7) and (8), the achievable rate of the legitimate user and the channel capacity of the eavesdropper are given by

$$R_B = \log_2 \left(1 + \frac{|\mathbf{h}_B^H \mathbf{w}_s|^2}{|\mathbf{h}_B^H \mathbf{w}_z|^2 + \sigma^2} \right) \quad (9)$$

and

$$C_E = \log_2 \left(1 + \frac{|\mathbf{h}_E^H \mathbf{w}_s|^2}{|\mathbf{h}_E^H \mathbf{w}_z|^2 + \sigma^2} \right), \quad (10)$$

respectively. Therefore, the achievable secrecy rate of the legitimate user is given by $R_S = (R_B - C_E)^+$, where $(x)^+ = \max(x, 0)$.

III. PROBLEM FORMULATION AND PROPOSED SOLUTION

In our considered system, our design aims to maximize the secrecy rate by optimizing the beam focusing vector and AN, i.e., \mathbf{w}_s and \mathbf{w}_z . To achieve this aim, we formulate the optimization problem as

$$\mathbf{P1} : \max_{\mathbf{w}_s, \mathbf{w}_z} R_S \quad (11a)$$

$$\text{s.t. } \|\mathbf{w}_s\|^2 + \|\mathbf{w}_z\|^2 \leq P, \quad (11b)$$

where (11b) denotes the transmit power constraint of the BS with the maximum transmit power P .

We next develop a low-complexity beam focusing scheme to transmit the information-carrying signal and AN for secrecy range maximization. We assume that the signal and AN beam focusing points, denoted by Q_S and Q_A , have the coordinates $L_S = (r_S \cos \theta_S, r_S \sin \theta_S)$ and $L_A = (r_A \cos \theta_A, r_A \sin \theta_A)$, respectively. Thus, the near-field channel from the BS to Q_S and Q_A are approximated as $\mathbf{h}_S \approx \tilde{\mathbf{h}}_S =$

$h_{S,\text{LoS}}\mathbf{h}^H(r_S, \theta_S)$ and $\mathbf{h}_A \approx \tilde{\mathbf{h}}_A = h_{A,\text{LoS}}\mathbf{h}^H(r_A, \theta_A)$, respectively, where $h_{S,\text{LoS}} = \frac{\lambda}{4\pi r_S} \exp(-\frac{1}{2}K(f)r_S)$, $h_{A,\text{LoS}} = \frac{\lambda}{4\pi r_A} \exp(-\frac{1}{2}K(f)r_A)$, and $\mathbf{h}^H(r_S, \theta_S)$ and $\mathbf{h}^H(r_A, \theta_A)$ are channel steering vectors of Q_S and Q_A , respectively.

For ease of implementation, we consider the maximum ratio transmission (MRT) based analog beam focusing for Q_S and Q_A , i.e., $\mathbf{w}_s = \sqrt{(1-\alpha)P} \frac{\mathbf{h}_S}{\|\mathbf{h}_S\|}$ and $\mathbf{w}_z = \sqrt{\alpha P} \frac{\mathbf{h}_A}{\|\mathbf{h}_A\|}$, to facilitate beam focusing, where $\alpha \in [0, 1)$ is the power allocation ratio on the AN. Given the correlation between any two near-field channel steering vectors, defined in [10, **Definition 1**], the correlations between the channel steering vectors of the legitimate user and Q_S , and between the channel steering vectors of the legitimate user and Q_A are given by

$$\rho_1 = \rho(r_B, \theta_B, r_S, \theta_S) = |\mathbf{h}^H(r_B, \theta_B)\mathbf{h}(r_S, \theta_S)| \quad (12)$$

and

$$\rho_2 = \rho(r_B, \theta_B, r_A, \theta_A) = |\mathbf{h}^H(r_B, \theta_B)\mathbf{h}(r_A, \theta_A)|, \quad (13)$$

respectively. Similarly, the correlations between the channel steering vectors of the eavesdropper and Q_S , and between the channel steering vectors of the eavesdropper and Q_A are given by

$$\rho_3 = \rho(r_E, \theta_E, r_S, \theta_S) = |\mathbf{h}^H(r_E, \theta_E)\mathbf{h}(r_S, \theta_S)| \quad (14)$$

and

$$\rho_4 = \rho(r_E, \theta_E, r_A, \theta_A) = |\mathbf{h}^H(r_E, \theta_E)\mathbf{h}(r_A, \theta_A)|, \quad (15)$$

respectively. It is worth noting that these correlations belong to a fixed interval, i.e., $\rho_i \in (0, 1]$, for $i = \{1, 2, 3, 4\}$. Accordingly, the achievable secrecy rate for $R_S > 0$ is rewritten as

$$\begin{aligned} R_S &= R_B - C_E \\ &= \log_2 \left(1 + \frac{|\mathbf{h}_B^H \mathbf{w}_s|^2}{|\mathbf{h}_B^H \mathbf{w}_z|^2 + \sigma^2} \right) - \log_2 \left(1 + \frac{|\mathbf{h}_E^H \mathbf{w}_s|^2}{|\mathbf{h}_E^H \mathbf{w}_z|^2 + \sigma^2} \right) \\ &= \log_2 \left(1 + \frac{(1-\alpha)P g_B \rho_1^2}{\alpha P g_B \rho_2^2 + \sigma^2} \right) - \log_2 \left(1 + \frac{(1-\alpha)P g_E \rho_3^2}{\alpha P g_E \rho_4^2 + \sigma^2} \right) \\ &= \log_2 \left(\frac{A+B}{A+C} \right), \end{aligned} \quad (16)$$

where $g_B = N|h_{B,\text{LoS}}|^2$, $g_E = N|h_{E,\text{LoS}}|^2$,

$$A = \alpha^2 P^2 \rho_2^2 \rho_4^2 g_B g_E + \alpha P \sigma^2 (\rho_2^2 g_B + \rho_4^2 g_E) + \sigma^2, \quad (17)$$

$$B = (1-\alpha)P \rho_1^2 g_B (\alpha P \rho_4^2 g_E + \sigma^2), \quad (18)$$

and

$$C = (1-\alpha)P \rho_3^2 g_E (\alpha P \rho_2^2 g_B + \sigma^2). \quad (19)$$

A. Beam Focusing Design

In this subsection, we determine the coordinates of both Q_S and Q_A for the signal and AN transmission to maximize the secrecy rate. Thus, the secrecy rate can be approximated as

$$\begin{aligned} R_S &\stackrel{(a)}{\approx} \log_2 \left(\frac{\alpha^2 P^2 \rho_2^2 \rho_4^2 g_B g_E + \alpha(1-\alpha)P^2 \rho_1^2 \rho_4^2 g_B g_E}{\alpha^2 P^2 \rho_2^2 \rho_4^2 g_B g_E + \alpha(1-\alpha)P^2 \rho_2^2 \rho_3^2 g_B g_E} \right) \\ &= \log_2 \left(\frac{\eta + \rho_1^2 / \rho_2^2}{\eta + \rho_3^2 / \rho_4^2} \right), \end{aligned} \quad (20)$$

where $\eta = \frac{\alpha}{1-\alpha} \geq 0$ and (a) is held by ignoring the noise power with respect to the received signal and AN power at both the legitimate user and the eavesdropper. To maximize the secrecy rate, it is essential that the received signal power at the legitimate user exceeds that at the eavesdropper, while the received AN power at the eavesdropper exceeds that at the legitimate user [10]. Based on it, the secrecy rate maximization problem can be approximated as

$$\max_{L_S, L_A} \log_2 \left(\frac{\rho_1^2}{\rho_3^2} \right) + \log_2 \left(\frac{\rho_4^2}{\rho_2^2} \right), \quad (21)$$

for a small η . We note that ρ_1 and ρ_3 depend solely on the coordinate of Q_S , L_S , while ρ_2 and ρ_4 depend solely on the coordinate of Q_A , L_A . Thus, the original optimization problem **P1** can be approximately decoupled to

$$\mathbf{P2}: \max_{L_S} \log_2 \left(\frac{\rho_1^2}{\rho_3^2} \right), \quad (22)$$

which maximizes the received signal power ratio between the legitimate user and the eavesdropper, and

$$\mathbf{P3}: \max_{L_A} \log_2 \left(\frac{\rho_4^2}{\rho_2^2} \right), \quad (23)$$

which maximizes the received AN power ratio between the eavesdropper and the legitimate user, regardless of the power allocation ratio, α . Since the received signal power at the legitimate user is maximized when $\theta_S = \theta_B$, and the received AN power at the eavesdropper is maximized when $\theta_A = \theta_E$ [10, **Proposition 1**], we adopt $\theta_S = \theta_B$ and $\theta_A = \theta_E$, and need to determine r_S and r_A to find the optimal Q_S and Q_A . With $\theta_S = \theta_B$ and [14, **Lemma 1**], ρ_1 and ρ_2 can be approximated as

$$\rho_1 \approx \left| \frac{C(\beta_1) + jS(\beta_1)}{2\beta_1} \right| \quad (24)$$

and

$$\rho_2 \approx \left| \frac{\tilde{C}(\beta_2, \beta_3) + j\tilde{S}(\beta_2, \beta_3)}{2\beta_3} \right|, \quad (25)$$

respectively, where $C(\beta) = \int_0^\beta \cos(\frac{\pi}{2}t^2) dt$ and $S(\beta) = \int_0^\beta \sin(\frac{\pi}{2}t^2) dt$ are Fresnel integrals, $\tilde{C}(\beta_2, \beta_3) = C(\beta_2 + \beta_3) - C(\beta_2 + \beta_3)$, $\tilde{S}(\beta_2, \beta_3) = S(\beta_2 + \beta_3) - S(\beta_2 + \beta_3)$, with $\beta_1 = \frac{N}{2} \sqrt{d \left| \frac{1}{r_B} - \frac{1}{r_S} \right|}$, $\beta_2 = (\theta_E - \theta_S) / \sqrt{d \left| \frac{1-\theta_E^2}{r_E} - \frac{1-\theta_S^2}{r_S} \right|}$, and $\beta_3 = \frac{N}{2} \sqrt{d \left| \frac{1-\theta_E^2}{r_E} - \frac{1-\theta_S^2}{r_S} \right|}$. Thus, the near-optimal $r_{S,\text{Opt}}$ is the solution to

$$\max_{r_S} \left(\frac{\beta_3^2 (C^2(\beta_1) + S^2(\beta_1))}{\beta_1^2 (\tilde{C}^2(\beta_2, \beta_3) + \tilde{S}^2(\beta_2, \beta_3))} \right), \quad (26)$$

which can be solved using the one-dimensional search method. Similarly, the near-optimal $r_{A,\text{Opt}}$ can also be obtained.

B. Power Allocation Design

We next determine the optimal power allocation ratio, α , in this subsection. We note that the signal and AN beam focusing design in Sec. III-A achieves the near-optimal secrecy

performance by ignoring the noise power, regardless of α . We now examine the effect of this noise power on the optimal power allocation ratio in our design.

Lemma 1: The optimal power allocation ratio to achieve the maximum secrecy rate is obtained as

$$\alpha = \begin{cases} \frac{-F_1 - \sqrt{F_1^2 - 4F_2F_0}}{2F_2}, & \text{if } F_0 > 0 \\ 0, & \text{otherwise,} \end{cases} \quad (27)$$

where F_0 , F_1 , and F_2 are given by

$$F_0 = P\sigma^2(P^2g_Bg_E\rho_1^2\rho_3^2(g_E\rho_4^2 - g_B\rho_2^2) + P\sigma^2(\rho_3^2\rho_4^2g_E^2 - \rho_1^2\rho_2^2g_B^2) + \sigma^4(\rho_3^2g_E - \rho_1^2g_B)), \quad (28)$$

$$F_1 = 2P^2g_Bg_E\sigma^2(Pg_B\rho_1^2\rho_2^2(\rho_3^2 - \rho_4^2) + Pg_E\rho_3^2\rho_4^2(\rho_2^2 - \rho_1^2) + \sigma^2(\rho_2^2\rho_3^2 - \rho_1^2\rho_4^2)), \quad (29)$$

and

$$F_2 = P^3g_Bg_E(Pg_Bg_E\rho_2^2\rho_4^2(\rho_2^2\rho_3^2 - \rho_1^2\rho_4^2) + g_B\rho_2^2\rho_3^2\sigma^2(\rho_2^2 - \rho_1^2) + g_E\rho_1^2\rho_4^2\sigma^2(\rho_3^2 - \rho_4^2)), \quad (30)$$

respectively.

Proof: Here, we define $\Omega = \frac{A+B}{A+C}$ and note that the maximum secrecy rate is achieved when Ω achieves its maximum value. To find the maximum value of Ω , we first evaluate the first derivative of Ω with respect to α as

$$\frac{\partial\Omega}{\partial\alpha} = \frac{F_2\alpha^2 + F_1\alpha + F_0}{(A+C)^2}. \quad (31)$$

Since the beam focusing design in Sec. III-A maximizes $\frac{\rho_1^2}{\rho_2^2}$ and $\frac{\rho_4^2}{\rho_3^2}$, it can be easily verified that F_2 and F_1 are always smaller than zero. Therefore, the monotonicity of Ω relies on the sign of F_0 . On the one hand, if $F_0 > 0$, Ω first increases and then decreases as α increases from 0 to 1. Thus, the maximum secrecy rate is achieved when $\frac{\partial\Omega}{\partial\alpha} = 0$. On the other hand, when $F_0 \leq 0$, $\frac{\partial\Omega}{\partial\alpha}$ is always smaller than zero, thereby resulting in a monotonically decreasing secrecy rate with respect to α . ■

Remark 1: We note that the AN helps improve the secrecy rate only when $F_0 > 0$ and the sign of F_0 primarily depends on the last term, i.e., $\rho_3^2g_E - \rho_1^2g_B$. Since g_E and g_B decrease when r_E and r_B increase, respectively, we find that the injection of the AN into signal transmission can improve the secrecy rate when the eavesdropper is located closer to the BS than the legitimate user, i.e., $g_E > g_B$. Otherwise, the improvement in the secrecy rate by the AN is limited. This will be illustrated in Sec. IV.

Finally, our proposed AN aided beam focusing scheme can be obtained by combining the signal and AN beam focusing design in Sec. III-A with the power allocation design in Lemma 1. Its benefits will be examined in Sec. IV.

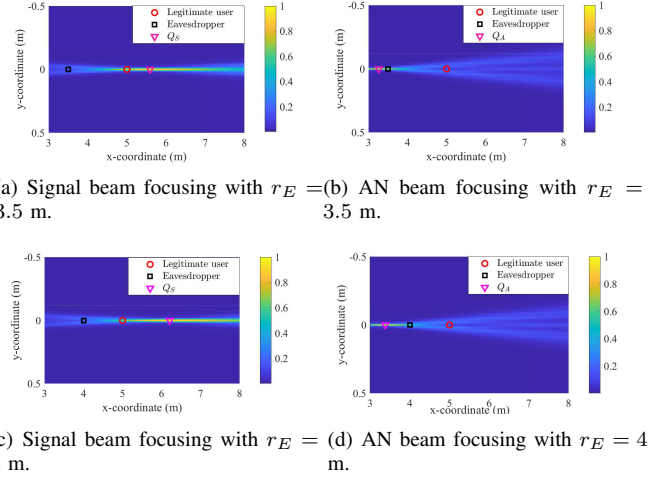


Fig. 2. The normalized signal power spectrum of the signal and AN beam focusing design with $r_B = 5$ m.

IV. NUMERICAL RESULTS

In this section, we present numerical results to demonstrate the effectiveness of our proposed AN aided beam focusing scheme in Sec. III. We set $N = 513$ antennas in the large-scale array, carrier frequency as $f = 300$ GHz, antenna spacing as $d = \lambda/2$, noise power as $\sigma^2 = -77$ dBm for a 5 GHz bandwidth, based on existing experimental platforms [15], transmit power as $P = 5$ dBm, the spatial angle from the x-axis to the legitimate user and the eavesdropper as $\theta_B = \theta_E = 0$, and the molecular absorption coefficient at frequency f as $K(f) = 0.00143$ m⁻¹. For comparison, we employ the state-of-the-art AN aided beam focusing scheme proposed in [10] as the benchmark scheme.

Fig. 2 plots the normalized signal power spectrum of the proposed signal and AN beam focusing design with $r_B = 5$ m and different r_E . We observe that the proposed Q_S and Q_A are not allocated to the legitimate user and the eavesdropper, respectively. Moreover, the distance between the legitimate user and the proposed Q_S , and that between the eavesdropper and the proposed Q_A , increase as the eavesdropper moves closer to the legitimate user. This observation is due to the two-fold impact on the secrecy rate when the distance from Q_S to the legitimate user and that from Q_A to the eavesdropper decrease. Specifically, the reduction in such distances increases both the received signal power at the legitimate user and the received AN power at the eavesdropper, as well as boosts the received signal power at the eavesdropper and the received AN power at the legitimate user, especially when the eavesdropper is close to the legitimate user. Importantly, this two-fold impact is addressed in our proposed beam focusing design.

Fig. 3 plots the secrecy rate, R_S , versus the power allocation ratio, α . We first observe that our proposed scheme achieves a higher secrecy rate than the benchmark scheme, which shows the superiority of our proposed scheme. We then observe that the optimal power allocation ratio derived in Lemma 1 achieves the optimal secrecy rate, demonstrating the accuracy of our analysis. We further observe that R_S first increases and then decreases as α increases. This observation is due to the fact that the increase in α has a two-fold impact on the secrecy

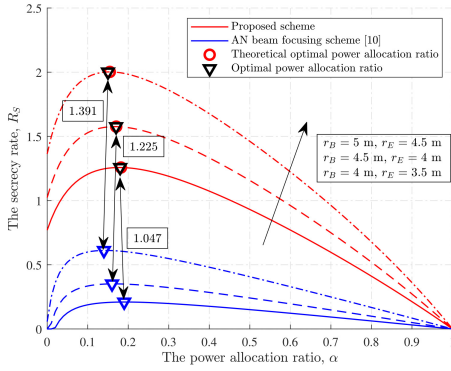


Fig. 3. The secrecy rate, R_S , versus the power allocation ratio, α .

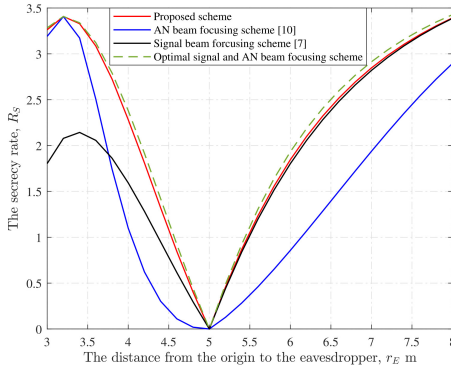


Fig. 4. The secrecy rate, R_S , versus the distance from the origin to the eavesdropper, r_E , with $r_B = 5$ m.

rate. Specifically, when α is small, its increase leads to a higher received AN power at the eavesdropper, thereby decreasing the channel capacity of the eavesdropper. However, once α exceeds a certain threshold, its increase leads to a profound decrease in the received signal power at the legitimate user, resulting in a lower channel capacity at the legitimate user and consequently the decreased secrecy rate.

Fig. 4 plots the secrecy rate, R_S , versus the distance from the origin to the eavesdropper, r_E , with $r_B = 5$ m. We can see that for all the schemes, the secrecy rate decreases and then increases as the distance from the origin to the eavesdropper, r_E , increases. This observation is due to the fact that the channels from the BS to the legitimate user and the eavesdropper are more similar when the eavesdropper is located close to the legitimate user, where this similarity significantly reduces the secrecy rate in near-field communication systems. The performance of our proposed scheme is very close to the optimal scheme. Additionally, our proposed scheme outperforms the AN beam focusing scheme in [10] and the signal beam focusing scheme in [7]. Compared to the scheme in [7], we find that our proposed scheme provides significant secrecy rate improvement when the eavesdropper is located closer to the BS than the legitimate user, i.e., $r_E < r_B$, while this improvement is not notable when the eavesdropper is located farther to the BS than the legitimate user, i.e., $r_E > r_B$. This observation is in accordance with Remark 1, which further validates our analysis. Note that the results for the optimal signal and AN beam focusing scheme are obtained by a numerical search method with the computational complexity $\mathcal{O}((NM)^3)$, where N is the number of antennas

and M is a constant that depends on the step size and/or the error threshold used in the one-dimensional search method. The computational complexity of the proposed scheme in [7] is $\mathcal{O}(N^3)$, while the computational complexity of our proposed scheme is only $\mathcal{O}(NM)$. Thus, our proposed scheme is computationally efficient compared to the benchmark schemes.

V. CONCLUSION

We proposed a novel design to safeguard information transmission for a single legitimate user against the risk of eavesdropping in a near-field THz communication system. By decoupling the original optimization problem, we solved each subproblem with a cost-cautious one-dimensional search method and derived the closed-form expression for the optimal power allocation ratio. We then combined the solutions to the two decoupled subproblems and devised a low-complexity AN aided beam focusing scheme to maximize the secrecy rate. Aided by numerical results, we demonstrated a significant performance gain achieved by the proposed scheme compared to the benchmark scheme, as well as discussed the insights arising from our proposed AN aided design.

REFERENCES

- [1] M. Giordani, M. Polese, M. Mezzavilla, S. Rangan, and M. Zorzi, "Toward 6G networks: Use cases and technologies," *IEEE Commun. Mag.*, vol. 58, no. 3, pp. 55–61, Mar. 2020.
- [2] N. Yang and A. Shafie, "Terahertz communications for massive connectivity and security in 6G and beyond era," *IEEE Commun. Mag.*, vol. 62, no. 2, pp. 72–78, Feb. 2024.
- [3] A. Shafie, N. Yang, C. Han, J. M. Jornet, M. Juntti, and T. Kürner, "Terahertz communications for 6G and beyond wireless networks: Challenges, key advancements, and opportunities," *IEEE Netw.*, vol. 37, no. 3, pp. 162–169, May 2023.
- [4] D. Bodet, V. Petrov, S. Petrushkevich, and J. M. Jornet, "Sub-terahertz near field channel measurements and analysis with beamforming and Bessel beams," *Sci. Rep.*, vol. 14, no. 19675, pp. 1–13, Aug. 2024.
- [5] J. Ferreira, J. Guerreiro, and R. Dinis, "Physical layer security with near-field beamforming," *IEEE Access*, vol. 12, pp. 4801–4811, Dec. 2024.
- [6] Z. Zhang, Y. Liu, Z. Wang, X. Mu, and J. Chen, "Physical layer security in near-field communications," *IEEE Trans. Veh. Technol.*, vol. 73, no. 7, pp. 10 761–10 766, Jul. 2024.
- [7] A. A. Nasir, "Max-min secrecy rate optimization through beam focusing in near-field communications," *IEEE Commun. Lett.*, vol. 28, no. 7, pp. 1594–1598, Jul. 2024.
- [8] V. Petrov, H. Guerboukha, A. Singh, and J. M. Jornet, "Wavefront hopping for physical layer security in 6G and beyond near-field THz communications," *IEEE Trans. Commun.*, pp. 1–1, 2024.
- [9] J. Chen, Y. Xiao, K. Liu, Y. Zhong, X. Lei, and M. Xiao, "Physical layer security for near-field communications via directional modulation," *IEEE Trans. Veh. Technol.*, vol. 73, no. 8, pp. 12 242–12 246, Aug. 2024.
- [10] Y. Zhang, Y. Fang, X. Yu, C. You, and Y.-J. A. Zhang, "Performance analysis and low-complexity beamforming design for near-field physical layer security," Jul. 2024. [Online]. Available: <https://arxiv.org/abs/2407.13491>
- [11] Y. Zhang, H. Zhang, S. Xiao, W. Tang, and Y. C. Eldar, "Near-field wideband secure communications: An analog beamfocusing approach," *IEEE Trans. Signal Process.*, vol. 72, pp. 2173–2187, Apr. 2024.
- [12] S. Liu, X. Yu, Z. Gao, J. Xu, D. W. K. Ng, and S. Cui, "Sensing-enhanced channel estimation for near-field XL-MIMO systems," Mar. 2024. [Online]. Available: <https://arxiv.org/abs/2403.11809>
- [13] Y. Zhang, X. Wu, and C. You, "Fast near-field beam training for extremely large-scale array," *IEEE Wireless Commun. Lett.*, vol. 11, no. 12, pp. 2625–2629, Dec. 2022.
- [14] J. Chen, F. Gao, M. Jian, and W. Yuan, "Hierarchical codebook design for near-field mmWave MIMO communications systems," *IEEE Wireless Commun. Lett.*, vol. 12, no. 11, pp. 1926–1930, Nov. 2023.

- [15] P. Sen, D. A. Pados, S. N. Batalama, E. Einarsson, J. P. Bird, and J. M. Jornet, "The teranova platform: An integrated testbed for ultra-broadband wireless communications at true terahertz frequencies," *Comput. Netw.*, vol. 179, p. 107370, Oct. 2020.